Thermoelectric property enhancement by Cu nanoparticles in nanostructured $FeSb_2$

Machhindra Koirala,[1] Huaizhou Zhao,[1,a)] Mani Pokharel,[2] Shuo Chen,[1] Tulashi Dahal,[1] Cyril Opeil,[2] Gang Chen,[3] and Zhifeng Ren[1,a)]
[1]*Department of Physics and TcSUH, University of Houston, Houston, Texas 77204, USA*
[2]*Department of Physics, Boston College, Chestnut Hill, Massachusetts 02467, USA*
[3]*Department of Mechanical Engineering, Massachusetts Institute of Technology, Cambridge, Massachusetts 02139, USA*

(Received 8 March 2013; accepted 14 May 2013; published online 29 May 2013)

We present the thermoelectric figure-of-merit (*ZT*) improvement in nanostructured $FeSb_2$ by Cu nanoparticles of ~5 nm as a modulation dopant. Because of the similar work functions between $FeSb_2$ and Cu and the high electrical conductivity of Cu, the Kondo insulator-like electrical resistivity of $FeSb_2$ at low temperatures was dramatically reduced. Both carrier concentration and mobility of the nanocomposites were improved over pure $FeSb_2$ without degrading the Seebeck coefficient. Overall, an improvement of ~90% in power factor was achieved for the optimized nanocomposite $FeSb_2Cu_{0.045}$. Combined with the reduced thermal conductivity by Cu/$FeSb_2$ interfaces, *ZT* was improved by ~110%. These results clearly demonstrate the potential of modulation doping to enhance the thermoelectric performance of $FeSb_2$. A similar approach could be applied to other Kondo insulators or previously known thermoelectric materials to improve *ZT*.
 [http://dx.doi.org/10.1063/1.4808094]

Cryogenic cooling (~77 K) using thermoelectric materials remains challenging so far, Kondo insulator and heavy fermion systems, such as CeB_6,[1] $YbAl_3$,[2] FeSi,[3] $FeSb_2$,[4–10] and $CrSb_2$ (Ref. 11) have been investigated for cryogenic cooling applications. However, the figure-of-merit (*ZT*), which determines the cooling efficiency, is much lower than those thermoelectric materials working at or above room temperatures. It is known that $ZT = (s^2\sigma/\kappa)T$, where *S*, σ, κ, and T are the Seebeck coefficient, electrical conductivity, thermal conductivity, and absolute temperature, respectively. Due to the large Seebeck *S* and high electrical conductivity σ observed in highly doped Kondo insulators and heavy fermions, large power factors (*PF*) have been reported. For example, $FeSb_2$ single crystals have a *PF* around $78 \times 10^{-4}\,W\,m^{-1}\,K^{-2}$ (Ref. 12) that is about twice the highest known *PF* when compared to other systems though it decreases to $5.5 \times 10^{-4}\,W\,m^{-1}\,K^{-2}$ for poly-crystal samples.[13] Most recently, it was reported $CrSb_2$ single crystal has *S* of $-5000\,\mu V\,K^{-1}$,[11] and p-type poly-crystal FeSi of $\sim 1200\,\mu V\,K^{-1}$.[3] In addition, doped FeSe[14] and $CeCu_6$ (Ref. 15) have also received attention for potential cryogenic application.

In addition to exploring new thermoelectric materials for cryogenic cooling applications, new approaches or strategies that can substantially improve the performance of the existing thermoelectric materials are also compelling. Recently, the approaches, such as nanostructures,[13,16–18] resonant doping,[19–21] band engineering at the Fermi level,[22,23] modulation doping that provides more charge carriers for higher electrical conductivity,[24,25] as well as metal/semiconductor interfacial engineering providing barrier to scatter phonons or improve *PF*[26–31] have been proved to be helpful in several material systems. In the case of strongly correlated materials, such as $FeSb_2$, nanostructures have been proved to be able to significantly increase *ZT*.[6,7,13]

In this report, inspired by the recent results, we achieved in $FeSb_{2-x}Ag_x/Ag_{1-y}Sb_y$ nanocomposite by adding Ag nanoparticles (NPs) into the system[32] and our early work on modulation doping in SiGe alloys,[24,25] we found that modulation doping approach substantially increases the *ZT* by ~110% through adding Cu NPs to make nanocomposite $FeSb_2$/Cu in which Cu nanoparticles act as the charge donor. This is a clear demonstration of modulation doping since the Cu does not diffuse into $FeSb_2$, this is distinct from our earlier study of SiGe alloys where significant amounts of B or P diffused easily into the parent compound,[24,25] which weakened the role of modulation doping. Similar work functions of the (100) planes in $FeSb_2$ and Cu facilitate the electron transfer from Cu to $FeSb_2$ at their interfaces to increase the electrical conductivity.

The $FeSb_2/Cu_x$ nanocomposites were synthesized by two procedures. For the synthesis of nanocomposites with ≤5 nm Cu nanoparticle inclusions, a total of 25 grams of Fe, Sb, and Cu with the stoichiometry of $FeSb_2Cu_y$ (y = 0.0225, 0.045, and 0.09) were mixed and sealed in vacuum in a quartz tube. Following a high temperature melt, quenching and 12 h of ball milling as previously reported,[13] 3 g of the ball milled powders with various amount of Cu nanoparticles (NPs) were pressed at 200 °C and 80 MPa for 2 min using direct current (dc) induced hot pressing method. For the synthesis of nanocomposites with ~100 nm Cu nanoparticle inclusion, $FeSb_2$ nanopowders were first prepared, then Cu NPs (~100 nm, Aldrich) were added into the powder with a final nominal composition of $FeSb_2Cu_{0.045}$. The mixed powders of ~5 g were further ball milled for 3 h. After this 3 h ball milling, some of the ~100 nm Cu particles may be milled to smaller nanoparticles, but should still be larger than ~5 nm. Disk samples were prepared by the same method mentioned above.

a)Authors to whom correspondence should be addressed. Electronic addresses: zhz0600@hotmail.com and zren@uh.edu

All the hot pressed samples with the same nominal composition $FeSb_2Cu_{0.045}$, but different sizes of Cu NPs, were characterized by high-resolution transmission electron microscopy (HRTEM) (JEOL 2010 F) for detailed structure and composition studies. The HRTEM samples were prepared by hand grinding and then dispersed in methanol, and the obtained suspension was dropped onto a typical carbon-coated Au grid, which can be used for HRTEM observation after drying. The edge area of the grains was selected for observations.

The temperature dependent electrical resistivity (ρ), Seebeck coefficient (S) and thermal conductivity (k) were measured on a Physical Property Measurement System (PPMS) from Quantum Design using the Thermal Transport Option (TTO). Gold leads were soldered onto samples with dimensions of $3 \times 3 \times 5$ mm^3. The normal 2-point TTO option of the PPMS for transport measurements was used. All the properties were measured in the direction perpendicular to the hot pressing direction.

The schematic band alignment between $FeSb_2$ and Cu, and the structure of $FeSb_2Cu_y$ nanocomposite are shown in Figs. 1(a) and 1(b), respectively. Since $FeSb_2$ is n-type semiconductor with a band gap of ~28 meV,[13] and its Fermi level located at the conduction band edge, the difference between the conduction band edge and vacuum level can be regarded as the same as the work functions for $FeSb_2$ at different crystal orientations. The work functions of $FeSb_2$ have been calculated to be 4.514 eV for (001) plane, 4.852 eV for (010) plane, and 4.723 eV for (100) plane.[32] According to the alignment of Fermi levels, the band bend for (001) and (010) planes, leaving an energy barrier in the range of 0.15–0.2 eV at their interfaces. However, due to the similar work functions between the (100) plane and Cu, which is 4.7 eV, the electron transfer between them would be much easier. It is reasonable to expect that Cu NPs can donate electrons from its conduction band to $FeSb_2$, which will increase the carrier concentration in the $FeSb_2$ host. Based on our early study, it appeared that the higher carrier concentration in nanostructured $FeSb_2$ mostly originated from its high defect density as compared to single crystal or micro sized samples.[13] As a result of the high defect density, the electrical conductivity of the nano sized $FeSb_2$ is significantly higher than the micro sized poly-crystal samples in the low temperature range (roughly $\leq$200 K), but the Seebeck coefficient is also significantly lower, which makes the power factor much lower. How to make the electrical conductivity in nanostructured $FeSb_2$ high without degrading the Seebeck coefficient is very challenging. We realized that localized Cu NPs can provide a large number of free electrons for higher electrical conductivity without changing the band structure of $FeSb_2$ for high Seebeck coefficient due to modulation doping similar to what was observed in SiGe alloy system.[24,25]

Fig. 2 shows the TEM images for both samples with the nominal composition of $FeSb_2Cu_{0.045}$. Figs. 2(a)–2(c) are for the samples prepared by mixing $FeSb_2$ nanopowder and ~100 nm Cu NPs, and Figs. 2(d) and 2(e) refer to samples in which Cu was incorporated by high temperature alloying resulting in very small Cu nanoparticles ~5 nm. In Fig. 2(a), we see the similar grain size and morphology for $FeSb_2$ host as we have shown in our previous reports.[13,32] It can be seen that the particle are composed of small size grains. Fig. 2(b) shows EDS (Energy Dispersive X-ray Spectroscopy) analysis of four selected areas. From regions A to D shown in Fig. 2(a), we see a transition from $FeSb_2$ to Cu, regions B and C are Cu dominated, and region D is approximately 200 nm, showing a slight aggregate of Cu. This indicates that Cu NPs are uniformly distributed in the composites. Region C in Fig. 2(a) is enlarged in Fig. 2(c), the measured lattice spacing from HRTEM images are 0.22 nm and 0.19 nm, which can be indexed to (111) and (200) planes of FCC Cu, respectively. Inverse Fast Fourier transform (IFFT) of the lattice image is also consistent with the Cu FCC structure with the [011] zone axis orientation. In Figs. 2(d) and 2(e), we observed that the size of Cu NPs is reduced to less than ~5 nm, while the $FeSb_2$ kept the similar size and morphology as that in Fig. 2(a). In terms of the volume ratio in both cases, Cu is about 0.9% in the host. The lattice spacing measurement and IFFT show that the $\sim 3 \times 3$ nm particle located at the edge area of $FeSb_2$ grains is Cu, due to the small size, EDS cannot focus on the Cu targets to confirm the composition. It is reasonable to assume that for the nanocomposites with smaller Cu particles, the Cu was first uniformly melted together with Fe and Sb when heated up to 1350 K. During cooling, Cu precipitates out as isolated nanoparticles due to the very limited solubility of Cu in $FeSb_2$.

The measured TE properties are shown in Fig. 3. Fig. 3(a) shows temperature dependence of thermal conductivity for all $FeSb_2Cu_y$ composites as well as the pure nanostructured $FeSb_2$. First, owing to the interfaces between Cu NPs and $FeSb_2$, reduced thermal conductivity was observed for

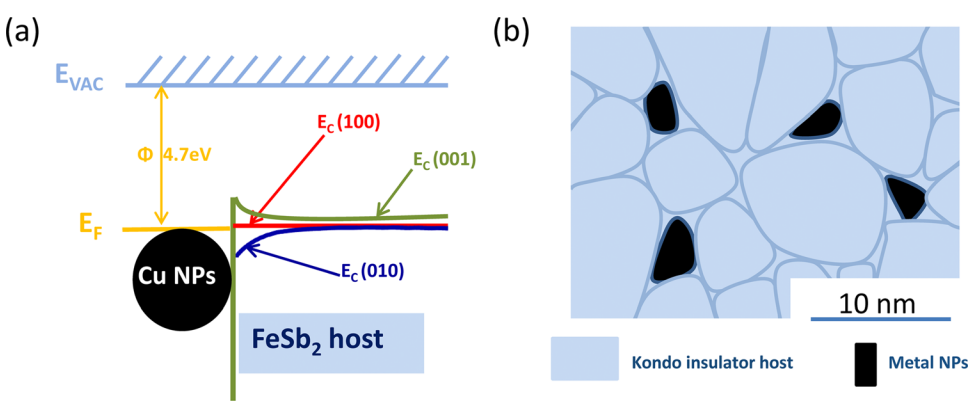

FIG. 1. Schematics of the band alignment between $FeSb_2$ and Cu (a); distribution of Cu NPs in the nanocomposite (b), scale bar indicates that the grains of $FeSb_2$ are around 50 nm on average and ~5 nm for Cu NPs.

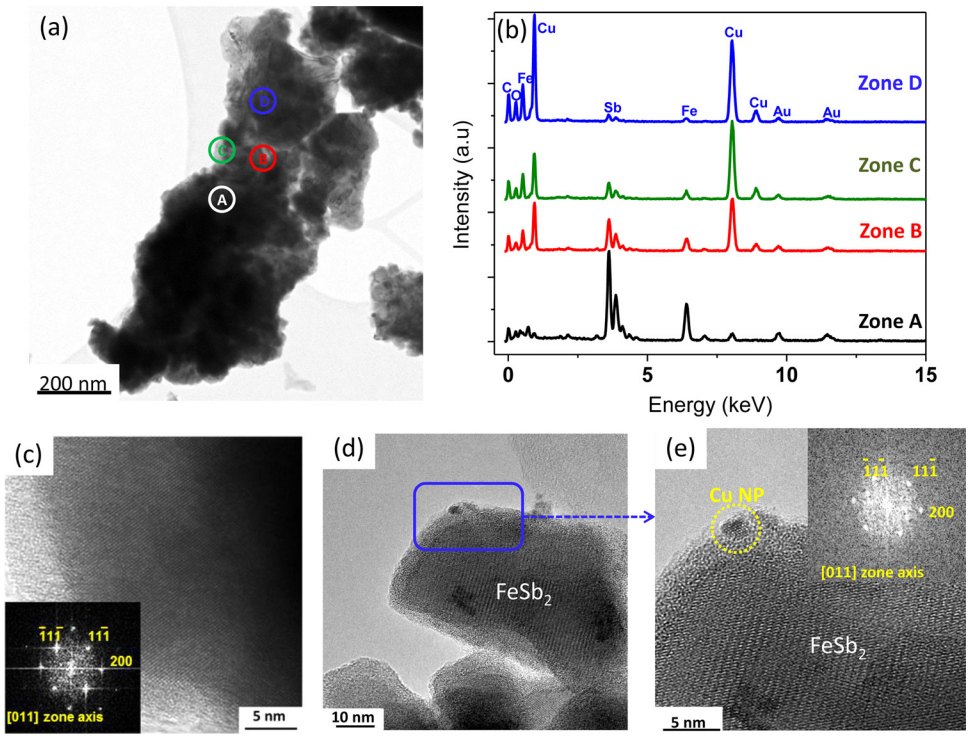

FIG. 2. TEM image (a) for $FeSb_2Cu_{0.045}$ nanocomposite prepared by mixing $FeSb_2$ nanopowder and 100 nm Cu NPs; (b) EDS for the selected zones in (a); (c) HRTEM for zone C shown in (a), inset shows IFFT for (c); (d) TEM image for $FeSb_2Cu_{0.045}$ nanocomposite prepared by melting Fe, Sb, and Cu at 1350 K and solidifying; and (e) is the enlarged area in (d), inset is the IFFT of the Cu nanoparticle area in (d).

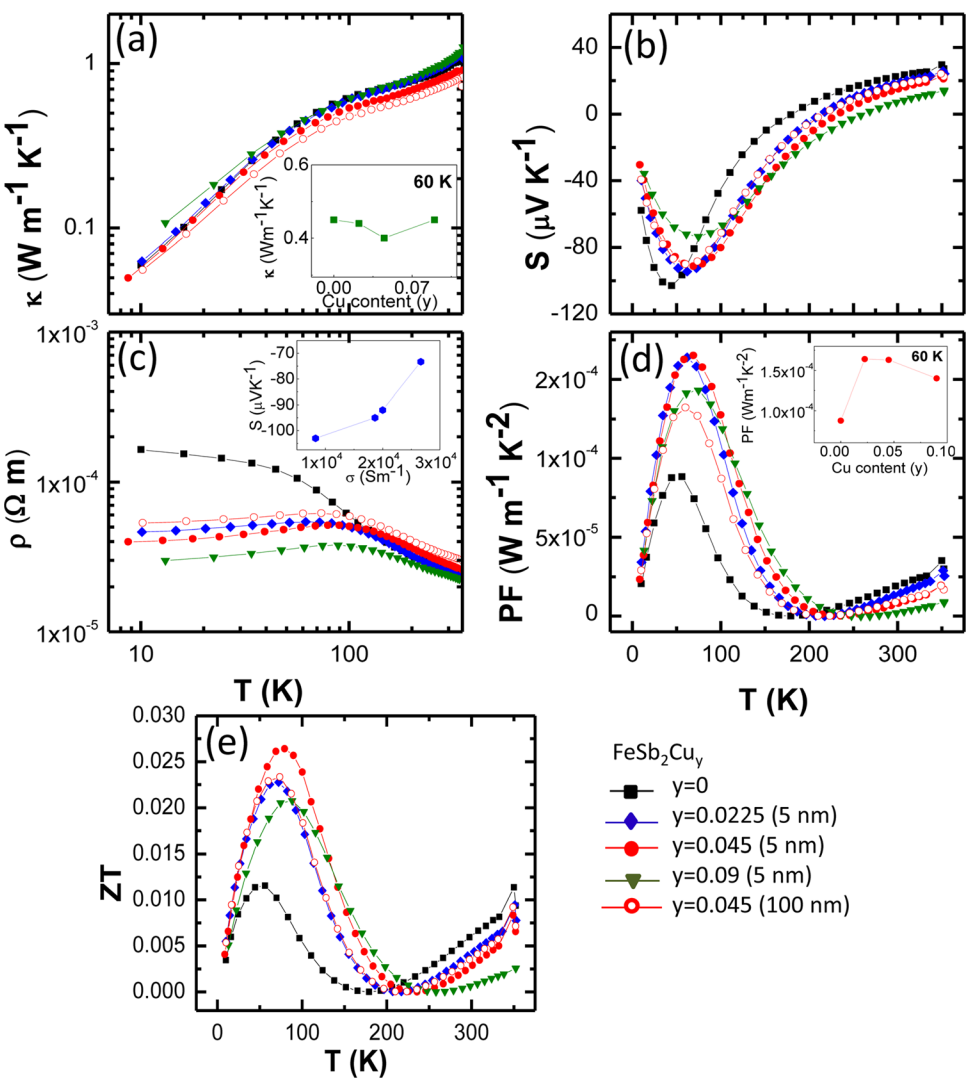

FIG. 3. Thermoelectric properties of $FeSb_2Cu_y$ ($y = 0$, 0.0225, 0.045, 0.09) samples: (a) temperature dependence of thermal conductivity, inset shows the measured thermal conductivity versus Cu content at 60 K; (b) temperature dependence of Seebeck coefficients; (c) temperature dependence of electrical resistivity, inset shows the peak Seebeck coefficient versus electrical conductivity at corresponding temperatures; (d) temperature dependence of power factor, inset shows the peak value of power factor at 60 K versus Cu content; and (e) temperature dependence of *ZT* for $FeSb_2$ and $FeSb_2Cu_y$ nanocomposites.

most samples. However, a notable difference between two $FeSb_2Cu_{0.045}$ samples was found, the one with larger Cu NPs (~100 nm) shows 20% lower thermal conductivity than that of pure $FeSb_2$ and 10% lower than the one with smaller Cu NPs (~5 nm). The former is understandable due to the interface phonon scattering, but the latter is very surprising and hard to understand at the moment. We guess the most possible reason is the subtle porosity difference between the two samples since our nanocomposites have relative density of 76% to 78%, as we have reported.[32]

As for all nanocomposites with ~5 nm Cu NPs, it is seen that with the increase of Cu content (inset of Fig. 3(a)), thermal conductivity at 60 K decreased slowly to a minimum of $0.39\,W\,m^{-1}\,K^{-1}$ for $FeSb_2Cu_{0.045}$ from $0.44\,W\,m^{-1}\,K^{-1}$ for the pure nanostructured $FeSb_2$. We believe that this is due to the phonon scattering at the interface of $FeSb_2$ and Cu. The minimum lattice thermal conductivity of $FeSb_2$ was reported to be $0.25\,W\,m^{-1}\,K^{-1}$ at 60 K,[33] indicating potential for further thermal conductivity reduction. When the Cu volume ratio reaches 1.8% for sample $FeSb_2Cu_{0.09}$, thermal conductivity becomes comparable to the pure nanostructured $FeSb_2$ and even larger below 50 K, which shows the contribution of increased electron thermal conductivity outweighs the decrease of the lattice thermal conductivity.

Seebeck coefficient results were shown in Fig. 3(b). Interestingly, the Seebeck coefficient only slightly decreases from $-102\,\mu V\,K^{-1}$ to $-93\,\mu V\,K^{-1}$ even though the electrical conductivity is increased by a factor of ~2 as shown is Fig. 3(c) for the $FeSb_2Cu_{0.045}$ sample with ~5 nm Cu NPs comparing to pure $FeSb_2$. The relatively high Seebeck coefficients at different concentrations of Cu nanoparticles can be understood as the result of modulation doping since the matrix $FeSb_2$ is not significantly affected.

Regarding the electrical conductivity shown in Fig. 3(c), we have achieved significant improvement by incorporating Cu NPs to the nanostructured $FeSb_2$. First, as temperature decreases, all the samples incorporated with Cu NPs show reduced electrical resistivity with metal-like features below 100 K compared to pure $FeSb_2$. Increasing the Cu content leads to reduced resistivity, while sample $FeSb_2Cu_{0.09}$ has the lowest resistivity. Clearly the $FeSb_2Cu_{0.045}$ sample having ~5 nm Cu NPs is more conductive than the samples with ~100 nm Cu NPs, probably due to better electron transfer from Cu to $FeSb_2$ when Cu is smaller and well dispersed in $FeSb_2$. Inset in Fig. 3(c) shows a peak Seebeck coefficient dependence of electrical conductivity for all nanocomposites with ~5 nm Cu NPs inclusion.

Because of the increased electrical conductivity and slightly reduced Seebeck coefficient for the $FeSb_2Cu_y$ nanocomposites, we observe a significant power factor *PF* improvement below 200 K for all Cu NPs incorporated nanocomposites compared to pure $FeSb_2$. As can be seen from Fig. 3(d)), a maximum $PF \sim 1.64 \times 10^{-4}\,W\,m^{-1}\,K^{-2}$ at 60 K was obtained for $FeSb_2Cu_{0.0225}$ before decreasing to $1.39 \times 10^{-4}\,W\,m^{-1}\,K^{-2}$ for $FeSb_2Cu_{0.045}$. Such a large improvement (~90%) over the pure $FeSb_2$ is comparable with the results achieved by other approaches such as resonant doping,[19–21] band engineering,[22,23] and modulation doping.[24,25] Combined with the slight decrease of thermal conductivity shown in Fig. 3(a), *ZT* of ~0.027 has been achieved, that is ~110% enhancement over ~0.013 achieved in the nanostructured pure $FeSb_2$ at 60 K.

In summary, we observed the figure-of-merit (*ZT*) improvement in nanostructured $FeSb_2Cu_y$ by modulation doping of Cu nanoparticles. Because of the favorable work functions between $FeSb_2$ and Cu nanoparticles, and the high electrical conductivity of Cu, the insulator-like electrical resistivity for $FeSb_2$ at low temperatures was reduced. It was found that the power factor was improved by ~90% and *ZT* ~110% for the optimized nanocomposite $FeSb_2Cu_{0.045}$ over the nanostructured pure $FeSb_2$. Our results suggest that a similar strategy could be extended to other Kondo insulators to enhance their TE properties if the modulation dopant does not severely react with the matrix.

The work was sponsored by Air Force Office of Scientific Research's MURI program under Contract No. FA9550-10-1-0533.

[1]S. R. Harutyunyan, V. H. Vardanyan, A. S. Kuzanyan, V. R. Nikoghosyan, S. Kunii, K. S. Wood, and A. M. Gulian, Appl. Phys. Lett. **83**(11), 2142 (2003).
[2]D. M. Rowe, M. Gao, and V. L. Kuznestsov, Philos. Mag. Lett. **77**(2), 105 (1998).
[3]B. C. Sales, O. Delaire, M. A. McGuire, and A. F. May, Phys. Rev. B **83**, 125209 (2011).
[4]A. Bentien, G. K. H. Madsen, S. Johnson, and B. B. Iversen, Phys. Rev. B **74**(20), 205105 (2006).
[5]A. Bentien, S. Johnsen, G. K. H. Madsen, B. B. Iversen, and F. Steglich, Europhys. Lett. **80**, 17008 (2007).
[6]P. Sun, N. Oeschler, S. Johnsen, B. B. Iversen, and F. Steglich, Phys. Rev. B **79**(15), 153308 (2009).
[7]P. Sun, N. Oeschler, S. Johnsen, B. B. Iversen, and F. Steglich, Dalton Trans. **39**, 1012 (2010).
[8]P. Sun, M. Søndergaard, Y. Sun, S. Johnsen, B. B. Iversen, and F. Steglich, Appl. Phys. Lett. **98**, 072105 (2011).
[9]M. S. Diakhate, R. P. Hermann, A. Möchel, I. Sergueev, M. Søndergaard, M. Christensen, and M. J. Verstraete, Phys. Rev. B **84**(12), 125210 (2011).
[10]A. Mani, J. Janaki, A. T. Satya, T. G. Kumary, and A. Bharathi, J. Phys.: Condens. Matter **24**, 075601 (2012).
[11]B. C. Sales, A. F. May, M. A. McGuire, M. B. Stone, D. J. Singh, and D. Mandrus, Phys. Rev. B **86**, 235136 (2012).
[12]Q. Jie, R. Hu, E. Bozin, A. Llobet, I. Zaliznyak, C. Petrovic, and Q. Li, Phys. Rev. B **86**(11), 115121 (2012).
[13]H. Z. Zhao, M. Pokharel, G. H. Zhu, S. Chen, K. Lukas, Q. Jie, C. Opeil, G. Chen, and Z. F. Ren, Appl. Phys. Lett. **99**, 163101 (2011).
[14]E. L. Thomas, W. Wong-Ng, D. Phelan, and J. N. Millican, J. Appl. Phys. **105**, 073906 (2009).
[15]A. Amato, D. Jaccard, J. Flouquet, F. Lapierre, J. L. Tholence, R. A. Fisher, S. F. Lacy, J. A. Olsen, and N. E. Phillips, J. Low Temp. Phys. **68**(5–6), 371 (1987).
[16]K. F. Hsu, S. Loo, F. Guo, W. Chen, J. S. Dyck, C. Uher, T. Hogan, E. K. Polychroniadis, and M. G. Kanatzidis, Science **303**(5659), 818 (2004).
[17]B. Poudel, Q. Hao, Y. Ma, Y. Lan, A. Minnich, B. Yu, X. Yan, D. Wang, A. Muto, D. Vashaee, X. Chen, J. Liu, M. S. Dresselhaus, G. Chen, and Z. F. Ren, Science **320**(5876), 634 (2008).
[18]X. Yan, G. Joshi, W. S. Liu, Y. C. Lan, H. Wang, S. Lee, J. W. Simonson, S. J. Poon, T. M. Tritt, G. Chen, and Z. F. Ren, Nano Lett. **11**, 556 (2011).
[19]J. P. Heremans, V. Jovovic, E. S. Toberer, A. Saramat, K. Kurosaki, A. Charoenphakdee, S. Yamanaka, and G. J. Snyder, Science **321**, 554 (2008).
[20]Q. Y. Zhang, H. Wang, W. S. Liu, H. Z. Wang, B. Yu, Q. Zhang, Z. T. Tian, G. Ni, S. Lee, K. Esfarjani, G. Chen, and Z. F. Ren, Energy Environ. Sci. **5**, 5246 (2012).
[21]J. P. Heremans, B. Wiendlocha, and A. M. Chamoire, Energy Environ. Sci. **5**, 5510 (2012).
[22]Y. Z. Pei, X. Y. Shi, A. LaLonde, H. Wang, L. D. Chen, and G. J. Snyder, Nature **473**, 66 (2011).
[23]Q. Zhang, F. Cao, W. S. Liu, K. Lukas, B. Yu, S. Chen, C. Opeil, D. Broido, G. Chen, and Z. F. Ren, J. Am. Chem. Soc. **134**, 10031 (2012).

[24]M. Zebarjadi, G. Joshi, G. H. Zhu, B. Yu, A. Minnich, Y. C. Lan, X. W. Wang, M. S. Dresselhaus, Z. F. Ren, and G. Chen, Nano Lett. **11**, 2225 (2011).
[25]B. Yu, M. Zebarjadi, H. Wang, K. Lukas, H. Z. Wang, D. Z. Wang, C. Opeil, M. S. Dresselhaus, G. Chen, and Z. F. Ren, Nano Lett. **12**, 2077 (2012).
[26]J. P. Heremans, C. M. Thrush, and D. T. Morelli, J. Appl. Phys. **98**, 063703 (2005).
[27]W. Kim, J. Zide, A. Gossard, D. Klenov, S. Stemmer, A. Shakouri, and A. Majumdar, Phys. Rev. Lett. **96**(4), 045901 (2006).
[28]S. V. Faleev and F. Léonard, Phys. Rev. B. **77**(21), 214304 (2008).
[29]M. Zebarjadi, K. Esfarjani, A. Shakouri, J.-H. Bahk, and Z. X. Bian, Appl. Phys. Lett. **94**, 202105 (2009).
[30]S. Sumithra, N. J. Takas, D. K. Misra, W. M. Nolting, P. F. P. Poudeu, and K. L. Stokes, Adv. Energy Mater. **1**, 1141 (2011).
[31]D. K. Ko, Y. J. Kang, and C. B. Murray, Nano Lett. **11**, 2841 (2011).
[32]H. Z. Zhao, M. Pokharel, S. Chen, B. Liao, K. Lukas, C. Opeil, G. Chen, and Z. F. Ren, Nanotechnology **23**, 505402 (2012).
[33]S. Zhu, W. J. Xie, D. Thompson, T. Holgate, M. H. Zhou, Y. G. Yan, and T. M. Tritt, J. Mater. Res. **26**(15), 1894 (2011).